Sensing Polymer/DNA Polyplex Dissociation Using Quantum Dot Fluorophores

Bingqi Zhang, Yanjie Zhang, Surya K. Mallapragada, and Aaron R. Clapp*

Department of Chemical and Biological Engineering, Iowa State University, Ames, Iowa 50011-2230, United States

ARTICLE

ABSTRACT We characterized the dissociation of polymer/DNA polyplexes designed for gene delivery using water-soluble quantum dots (QDs). A pH-responsive pentablock copolymer was designed to form stable complexes with plasmid DNA *via* tertiary amine segments. Dissociation of the polyplex was induced using chloroquine where the efficiency of this process was sensed through changes in QD fluorescence. We found that increasing concentrations of pentablock copolymer and DNA led to quenching of QD fluorescence, while chloroquine alone had no measurable effect. The mechanism of quenching was elucidated by modeling the process as the combination of static and dynamic quenching from the pentablock copolymer and DNA, as well as self-quenching due the bridging of QDs. Tertiary amine homopolymers were also used to study the effect of chain length on quenching. Overall, these QDs were found to be highly effective at monitoring the dissociation of pentablock copolymer/DNA polyplexes *in vitro* and may have potential for studying the release of DNA within cells.

KEYWORDS: gene delivery · DNA · polyplex · chloroquine · quantum dots · FRET

Semiconductor quantum dots (QDs) have seen increasing use in conjunction with or as an alternative to organic fluorophores in molecular and cellular imaging for nonviral gene delivery due to their broad excitation spectra, narrow and size-tunable emission spectra, and superior brightness and photostability.[1,2] QDs can be coupled either to polymers or DNA to investigate intracellular trafficking of the target particles among stained organelles.[3−8] In particular for measuring polymer−DNA interactions, the distance between polymer and DNA can be sensed by Förster resonance energy transfer (FRET) in which QDs function as fluorescence energy donors.[9−11] However, regardless of method used, appropriate chemical modifications are required, either for QDs, DNA, or other DNA condensing agents, which leads to complicated processing and/or potential interference with the functionality of the biomolecules or nanocrystals. Here, we report for the first time a facile and sensitive method to examine unpacking of polymer−DNA polyplexes induced by other competing agents on the basis of QD quenching.

We have developed a promising new thermogelling cationic pentablock copolymer vector for sustained gene delivery.[12,13] In addition to favorable transfection efficiencies and low cytotoxicity, these vectors exhibited a selectivity for transfection of cancer cells *versus* noncancer cells;[14] however, the mechanism behind this selectivity is not fully understood. There have been several studies aimed at elucidating the intracellular mechanism of gene transfection for various polymeric vectors by trafficking studies and other methods.[15−17] The ability to track the dissociation of polymer−DNA complexes intracellularly would provide answers to the key questions regarding vector unpackaging and its effect on transfection efficiency. As a common lysosomotropic agent, chloroquine (CLQ) has been found to significantly enhance transfection efficiency in many systems.[18−20] Among the multiple roles CLQ may play in assisting gene delivery, facilitating dissociation of DNA from polymers has emerged as an interesting possibility as it is also helpful for evaluating intracellular gene delivery barriers.[21] The main strategy currently used by researchers to measure CLQ-triggered polyplex dissociation relies on intercalating DNA dyes, either by measuring the amount of released DNA following removal of intact polyplexes through membrane filtration[22,23] or through a dye exclusion assay presuming that polyplex dissociation can be characterized by the susceptibility of DNA to dye intercalation.[23] However, one essential problem in these methods is that the intercalating capacity of CLQ with DNA can compete with many of the dyes used for DNA quantification, making it extremely difficult to accurately measure the actual amount of

*Address correspondence to clapp@iastate.edu.

Received for review August 3, 2010 and accepted December 13, 2010.

Published online December 29, 2010.
10.1021/nn1018939

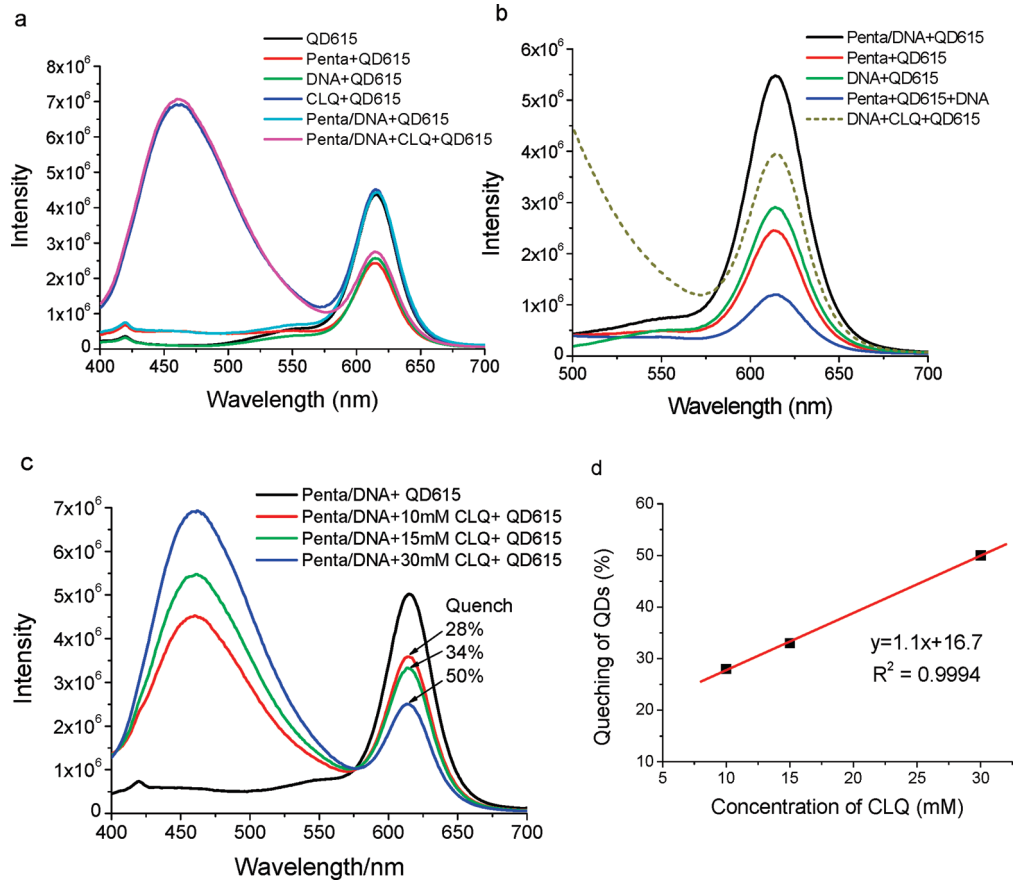

Figure 1. (a) Fluorescence spectra showing the influence of pentablock copolymer (penta), DNA, CLQ, and penta/DNA polyplex on the fluorescence emission of QD615. (b) Fluorescence spectra showing the influence of penta, DNA, and polyplex on the fluorescence emission of QD615. (c) Influence of CLQ when polyplex and QD615 are mixed together. (d) Plot of QD615 quenching *versus* CLQ concentration generated from the data in (c).

free DNA in solution or to assess the displacing effect of CLQ. In this work, we utilize cysteine-coated CdSe−ZnS core−shell QDs in place of common DNA intercalating dyes to measure DNA released from dissociation of polyplexes formed with DNA and poly(diethylaminoethylmethacrylate) (PDEAEM)/Pluronic F127 pentablock copolymers in the presence of CLQ.

RESULTS AND DISCUSSION

Polyplex Dissociation Monitored by QD Fluorescence Quenching. CdSe QDs have been reported to bind molecules having tertiary amines with high affinity.[24] Though not previously demonstrated, hydrophilic Cys-capped CdSe−ZnS QDs were considered as viable binding surfaces for the pentablock copolymers (having similar blocks of tertiary amines) used in this work. Interestingly, pentablock copolymers induced significant quenching of QD fluorescence upon mixing. QDs mixed with plasmid DNA led to similar quenching effects, but to a lesser extent. In contrast, the quenching effect was completely absent when QDs were mixed with preformed pentablock copolymer/DNA (penta/DNA) polyplexes, as shown in Figure 1a (black and light blue curves). The dramatic difference in QD fluorescence intensity between bound and unbound states of pentablock copolymer and DNA suggested that polyplex association/dissociation might function as a potential "on/off" switch for QD fluorescence (illustrated in Figure 2). CLQ alone was found not to influence the emission profile of the QDs studied (QDs having an emission maximum at 615 nm, or QD615), though CLQ itself demonstrated an intense and broad emission between 400 and 575 nm when excited at 370 nm (Figure 1a, dark blue and pink curves). Thus, we were able to investigate the stability of the polyplex in the presence of CLQ by monitoring the change in QD fluorescence where any decrease in the intensity of QD emission is attributed to polyplex dissociation.

As expected, addition of CLQ to solutions containing penta/DNA polyplex and QDs resulted in significant quenching of QDs when compared with control samples lacking CLQ. This provides a strong indication that CLQ indeed facilitated polyplex dissociation. The newly released pentablock copolymers appear to quench QDs immediately once they are free in solution. Released DNA is partially complexed with CLQ and therefore exhibits relatively weaker quenching effects with QDs as compared to naked DNA mixed with QDs, as shown in Figure 1b. When pentablock copolymer and DNA were mixed with QDs *sequentially* (*i.e.*, penta-

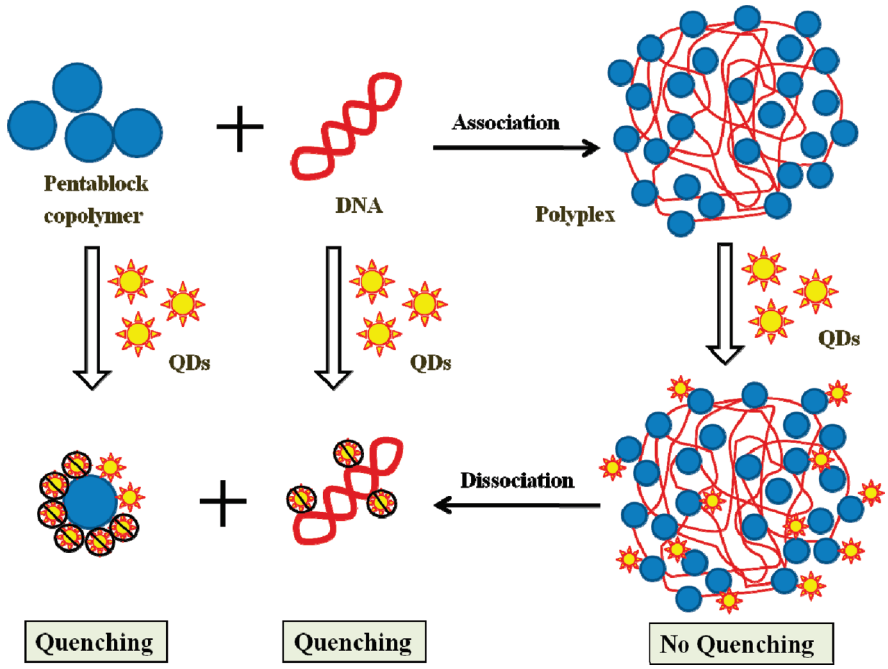

Figure 2. Schematic illustration of the mechanism of sensing pentablock copolymer/DNA polyplex dissociation using QDs. QDs can be quenched by the free pentablock copolymer and/or free DNA, but not by penta/DNA polyplex. Once polyplex dissociates, the released pentablock copolymer and DNA will lead to QD quenching in such a way that polyplex dissociation can be monitored with the decrease in QD fluorescence.

block copolymer added to QD solution, followed by the addition of DNA), allowing time to equilibrate between additions, there was increased quenching of QDs over the effect achieved with either component alone. This indicates the pentablock copolymer and DNA did not significantly associate into polyplexes when introduced serially to a solution containing QDs. The combined quenching effects provide further evidence for association of pentablock copolymer and QDs *via* tertiary amines since these amine groups would otherwise interact with the phosphate groups of DNA to form polyplexes and partially restore the original fluorescence of QDs. Therefore, the quenching observed in a polyplex solution after addition of CLQ likely results from both free pentablock copolymer and CLQ-bound/free DNA. The overall quenching of QD fluorescence exhibited a linear relationship with the concentration of CLQ, as shown in Figures 1c,d, further confirming the feasibility of using QDs to indicate polyplex dissociation induced by CLQ.

Although this study focused on cell-free assays, the CdSe−ZnS QDs used in this work showed no measurable acute toxicity in various cell lines due in part to a protective shell and dense coating of hydrophilic DTC-Cys ligands. The QD-based quenching method can thus be utilized to sense polyplex dissociation in cellular environments. For example, by co-incubating polyplexes and QDs with cells, dissociation of polyplexes in endosomes could be detected, which is of great importance for understanding the mechanism of gene delivery and improving transgene vectors. Furthermore, since the QDs were rendered water-soluble through ligand exchange, various types of amino acids can be easily coupled to QDs as designed; for example, histidine residues can be coupled to the surface of QDs, leading them to readily escape endosomes. In this case, polyplex dissociation can be monitored by quenching of QDs throughout the cytoplasm.

Quantitative Models of Fluorescence Quenching. Since the pentablock copolymer potentially acts as the primary quenching species, we expect the QD fluorescence to decrease (and thereby quenching to *increase*) with increasing polymer concentration. As shown in Figure 3a, the measured QD fluorescence intensity showed an inverse dependence on the concentration of pentablock copolymer. Rather than exhibiting a linear dependence on concentration consistent with either static or dynamic quenching alone, the integrated quenching data appeared concave up (Figure 3b), suggesting a combination of quenching effects. We fit these data with a modified Stern−Volmer equation that describes combined dynamic and static quenching (Figure 3b, dashed line) in which static quenching is presumed to occur when the quencher is within a characteristic radius (spherical volume) consistent with a stable complex:[25]

$$F_0/F = (1 + K_D[Q])\exp([Q]V) \quad (1)$$

where

$$V = V_0 N_A/1000 \quad (2)$$

Here, F_0 and F are the fluorescence intensities in the absence and presence of quencher, respectively; K_D is the dynamic quenching constant; $[Q]$ is the concentration

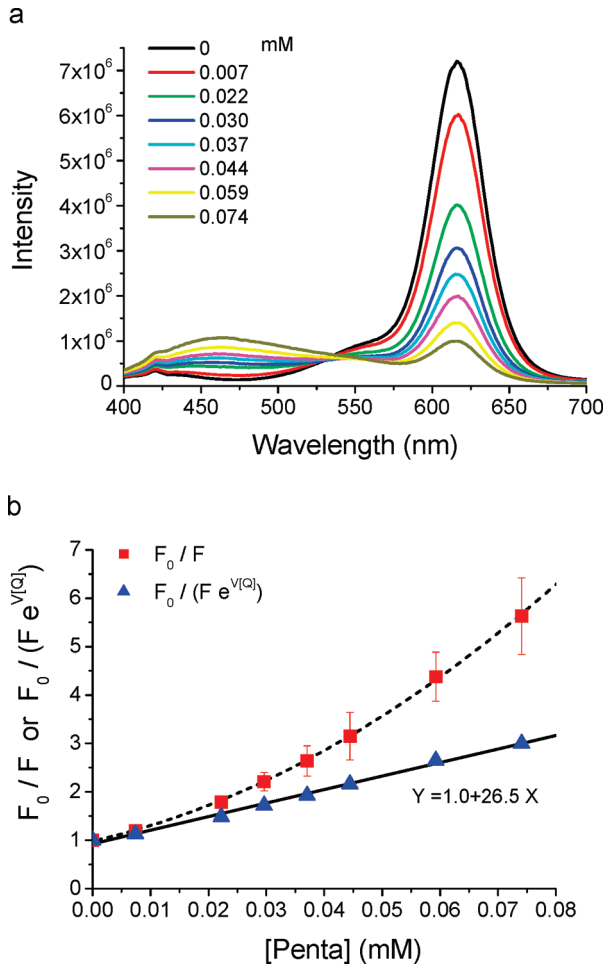

Figure 3. Quenching of QD as a function of concentration of the pentablock copolymer (penta): (a) fluorescence spectra and (b) integrated quenching using two models.

of quencher (pentablock copolymer in this experiment); V is the molar volume of the sphere within which the probability of quenching is unity; V_0 is the volume of the sphere in cm^3; and N_A is the Avogadro constant. The fitted sphere volume was consistent with an interaction radius of 15 nm. Alternatively, a plot of $F_0/(Fe^{[Q]V})$ *versus* [Q] yields a straight line with the slope equal to K_D, which is found to be about 26.5 mM^{-1} (Figure 3b, solid line).

In order to interpret this result, we measured the size distribution of QD−pentablock copolymer assemblies (micelles) in solution using dynamic light scattering. The data showed nearly monodisperse micelles having a mean diameter of 200 nm (polydispersity index, PDI = 0.062). On the basis of this size distribution and the average QD diameter (~15−20 nm), there are presumably many QDs within each micelle. This physical arrangement suggests that QDs are likely to exhibit interparticle energy transfer (*i.e.*, FRET) which would contribute to the static quenching component of the Stern−Volmer model shown in eqs 1 and 2. The fitted interaction radius will then be representative of the composite effect of FRET-induced quenching as well as any direct quenching due to the pentablock copolymer alone. If FRET is a significant quenching mechanism, we expect the fitted interaction radius to be on the same order as the Förster distance for QD self-quenching ($R_0 \sim 4-8$ nm), which is considerably smaller than the average micelle size ($r_m \sim 100$ nm). The modified Stern−Volmer model alone is insufficient to determine the relative static quenching contribution of QD self-quenching versus direct quenching from the polymer. For this, we require experiments that isolate these effects; this is the subject of the next section.

In the case of QD quenching by DNA, again there is enhanced quenching with increasing DNA concentration, yet the data are concave down (Figure 4a,b), consistent with a fluorophore having accessible and inaccessible populations to the quencher and a fit to the following equation:

$$F_0/\Delta F = 1/f_a K_a[Q] + 1/f_a \quad (3)$$

where

$$\Delta F = F_0 - F \quad (4)$$

$$f_a = F_{0a}/F_0 \quad (5)$$

Here, F_0 and F again refer to the fluorescence in the absence and presence of quencher, respectively; f_a is a fraction of the total fluorophore population where the subscript *a* refers to the accessible fraction that can be deactivated by the quencher species; correspondingly, F_{0a} is the initial fluorescence and K_a is the quenching constant of the accessible fraction. For the mechanism of quenching by DNA, guanine bases are thought to be responsible as electron donors.[25] Since plasmid DNA cannot maintain its circular structure but rather contorts into a supercoiled conformation in aqueous solution, the guanine bases would assume a complex distribution of accessibilities to the QD surface. As a result, it might be difficult for larger QDs to contact these quenching sites as compared to smaller QDs. Thus we assumed that only a fraction of QDs were available to be quenched by DNA. Values for f_a and K_a can be obtained readily from the intercept and slope by plotting $F_0/\Delta F$ *versus* [Q]$^{-1}$ (Figure 4c), which were found to be 0.62 and 0.14 μL/μg, respectively.

Self-Quenching among QDs. Considering that both pentablock copolymer and DNA have the capacity to associate with QDs, they could feasibly generate a high local concentration of QDs and initiate self-quenching. The tendency of pentablock copolymer to form micelles in solution furthers the speculation that QD self-quenching is an important mechanism in these systems. In order to test this hypothesis, we examined the quenching of two distinct populations of QDs, QD519 (green emitting) and QD611 (red emitting), that can potentially form FRET donor−acceptor pairs between QDs, as reviewed by Somers *et al.*[26] If such a pair is formed in proximity sufficient for energy transfer (*i.e.*,

on the order of the Förster distance R_0), we expect to see an increase in the ratio of red to green QD fluorescence (favorable quenching of the higher energy fluorophores). In order to elucidate the functional moieties responsible for the quenching behavior of the pentablock copolymer, a family of poly(dimethylaminoethylmethacrylate) (PDEAEM) homopolymers and Pluronic F127 were included in the study. These polymers comprise the end blocks and core triblock segments of the pentablock copolymer, respectively. As shown in Figure 5, pentablock copolymers and PDEAEM homopolymers preferentially quenched QD519 (higher QD611/QD519 photoluminescence ratio), whereas DNA quenched each QD population about equally (ratio near 1.0). Conversely, Pluronic F127 had no measurable effect on the QD emission spectra (data not shown), indicating that the core triblock structure (PEO_{100}-*b*-PPO_{65}-*b*-PEO_{100}) played no direct role in the quenching achieved with the full pentablock copolymer. The terminal PDEAEM blocks on pentablock copolymer are therefore likely to be the essential functional segments responsible for QD quenching, either by directly deactivating fluorescence relaxation pathways or aggregating QDs together. Notably, PDEAEM homopolymers exhibited variable quenching effects depending on polymerization degree (*i.e.*, molecular weight). Although we observed greater quenching in the QD519 population as compared to QD611 for all polymers, this result alone is insufficient to demonstrate energy transfer from QD519 to QD611 unless isolated control populations of QD519 have an equal or lesser tendency to be quenched in the presence of polymer than QD611. To this end, we studied these two populations of QDs separately and found that QD611 was more readily quenched by pentablock and PDEAEM homopolymers than QD519 (Figure 6), which contrasts the observations using mixed QD populations and provided compelling evidence of energy transfer from QD519 to QD611. The quenching data shown in Figures 5c and 6c were combined into one graph to summarize the differences in polymer-induced quenching behavior between isolated and mixed QD samples. The normalized quenching ratio, $(Q_{611}/Q_{519})_{mixed}/(Q_{611}/Q_{519})_{separate}$, was calculated and shown in Figure 7, where ratios below 1.0 correspond to preferred quenching of the QD519 population in mixed QD samples, as is expected from Förster theory. From these data, we can conclude that FRET is the dominant quenching mechanism for QDs exposed to pentablock copolymers in solution. Similarly, PDEAEM homopolymers also showed capacity to facilitate self-quenching (Figures 5c and 6c) and preferential QD519 quenching in mixed samples, as summarized in Figure 7. As the polymerization degree of homopolymer increased from 15 to 35, the overall quenching increased slightly and would presumably continue to increase as the molecular weight increased further.

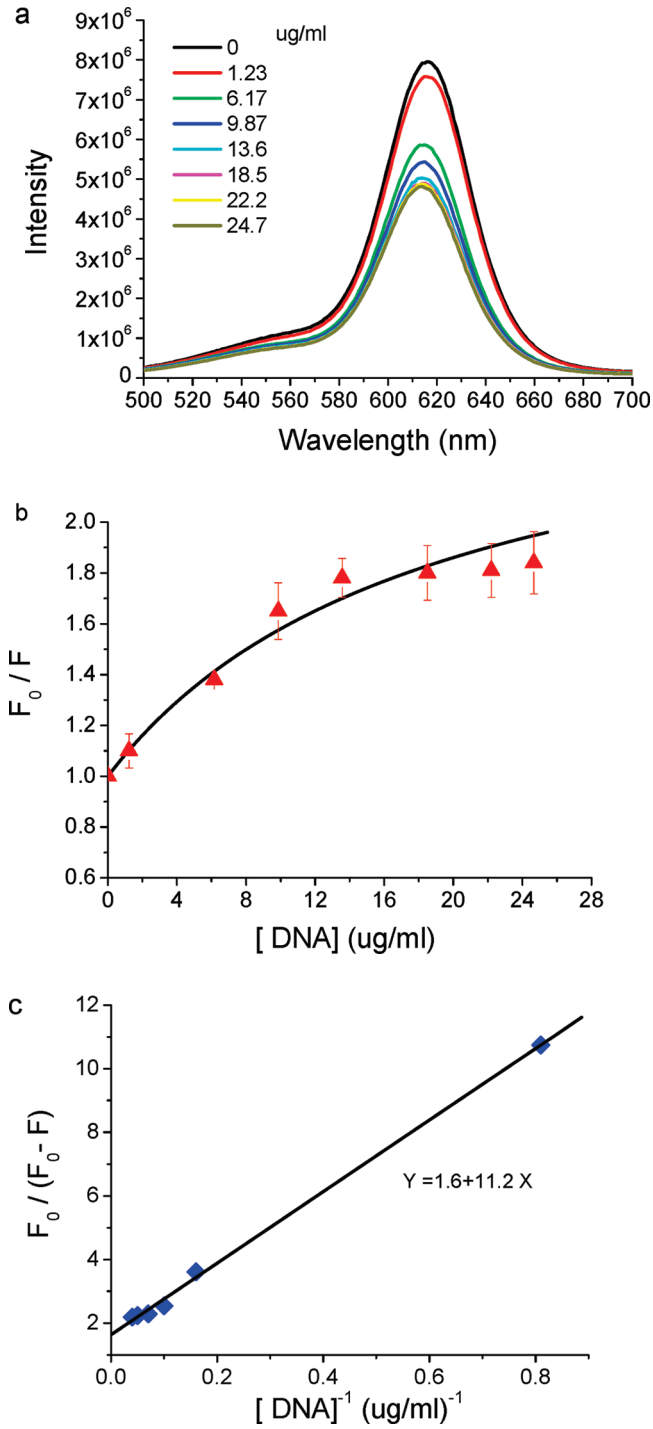

Figure 4. Fluorescence emission/quenching of QD as a function of DNA: (a) measured QD emission spectra, (b) integrated QD quenching (F_0/F), (c) normalized quenching *versus* inverse DNA concentration fit with a linear quenching model.

In particular, the pentablock copolymer led to nearly complete quenching of QDs when the concentration of PDEAEM block was as high as that in other homopolymers (Figure 6b), suggesting pentablock copolymers are more efficient at quenching QDs compared to homopolymers when holding the total mass of available PDEAEM constant. This is notable because the core triblock Pluronic F127 alone showed no

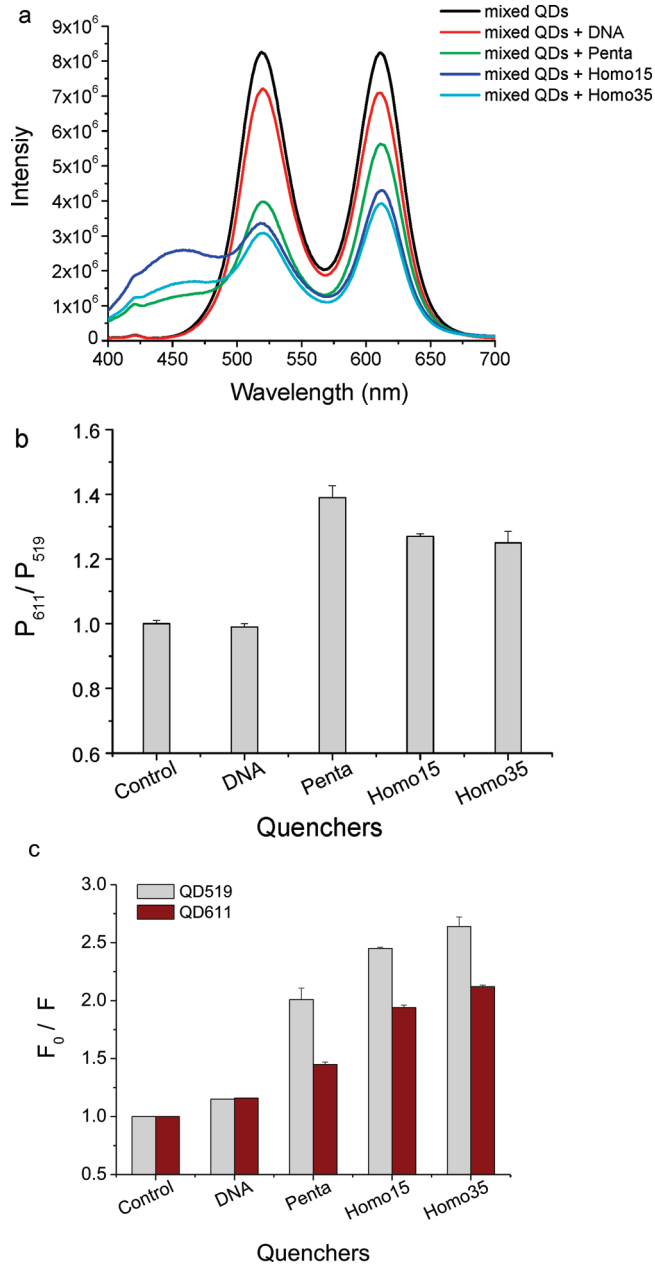

Figure 5. Quenching of two mixed populations of QDs by DNA, pentablock copolymer (penta), and poly(dimethylaminoethylmethacrylate) homopolymers with polymerization degree of 15 (Homo15) and 35 (Homo35). (a) Fluorescence spectra of QD519 and QD611 (initially having similar intensities) mixed with various polymers. (b) Calculated ratios of the peak QD heights (QD611/QD519) shown in (a). (c) Degree of quenching for both QD519 and QD611 as a function of polymer type.

quenching effect with QDs whatsoever. In an effort to elucidate the mechanism of quenching initiated by different polymers, varying amounts of PDEAEM homopolymers having degrees of polymerization of 15 (Homo15) and 35 (Homo35) were mixed with QDs to study quenching as a function of concentration. As shown in Figure 8, the relationship between quenching extent and homopolymer concentration was well-described by the same Stern−Volmer model (eqs 1 and 2) used to characterize pentablock copolymer-induced quenching, indicating that homo- and pentablock polymers share a similar mechanism of QD quenching. However, the fitted quenching constants, K_D, for Homo15 and Homo35 were found to be 0.85 and 4.7 mM^{-1}, respectively, far lower than the 26.5 mM^{-1} value measured using pentablock copolymer. The unique micellar structure of pentablock copolymers in solution likely accounts for this discrepancy where several QDs can bind each micelle thus facilitating and enhancing self-quenching.

FRET-induced fluorescence quenching is expected to show strong wavelength dependence due to variations in donor−acceptor spectral overlap. In our study, all PDEAEM-containing polymers showed obvious wavelength-dependent quenching behavior when mixed with QDs. Quenching measured as a function of

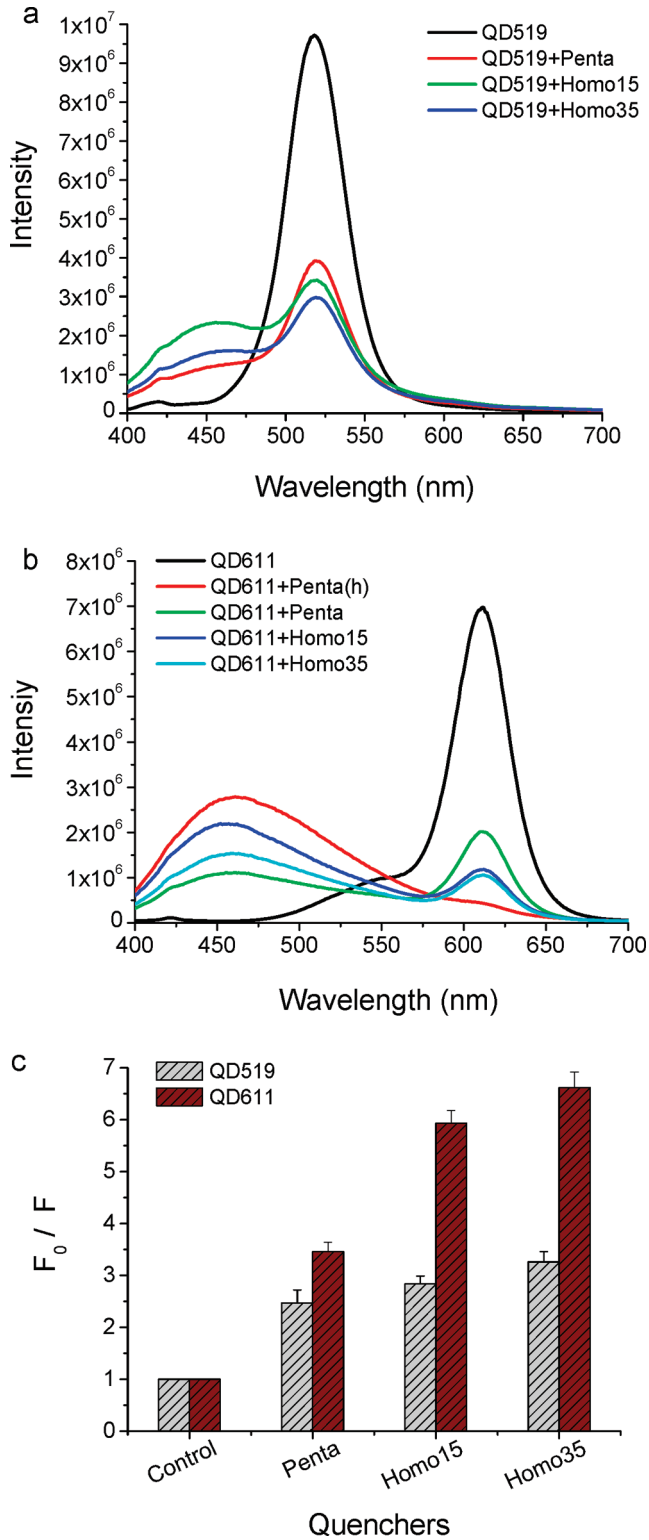

Figure 6. Fluorescence emission spectra indicating quenching of separate populations (a) QD519 and (b) QD611 by pentablock copolymer (penta) and poly(dimethylaminoethylmethacrylate) homopolymers with polymerization degree of 15 (Homo15) and 35 (Homo35) at concentration of 2 mg/mL. Penta(h) in (b) refers to a high concentration of pentablock copolymer containing the same amount of PDEAEM as in other homopolymers. The quenching efficiency was given as F_0/F and is depicted in (c).

wavelength (Figure 9) appeared similar in shape to a plot of the spectral overlap function from Förster theory, $J(\lambda)$ (not shown), which considers the QD emission and absorption spectral overlap; this further implicates a QD-to-QD self-quenching mechanism. Static quenching could also occur through complexation between the pentablock copolymer and QDs, although this type of quenching typically shows little depen-

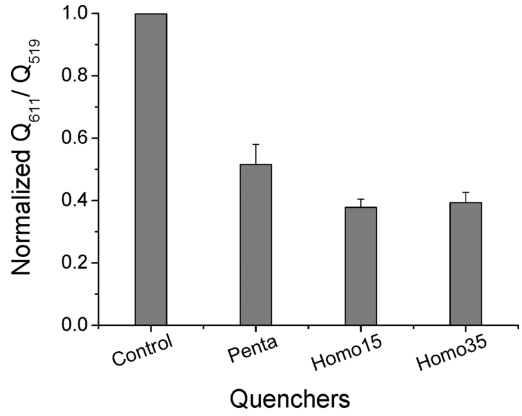

Figure 7. Normalized ratio of quenching of QD611 (Q_{611}) to quenching of QD519 (Q_{519}) in mixed samples. *Q* denotes quenching extent, defined as F_0/F; normalization was achieved by dividing the ratio of Q_{611}/Q_{519} for mixed QDs by the ratio for separate QDs. The normalized ratio indicates quenching by energy transfer between QD611 and QD519 in mixed QD samples, where a value <1.0 is consistent with preferential quenching of the QD519 population (which was true for all three polymer tested).

dence on wavelength, as in a recent example of static quenching of QDs by Medintz *et al.*[27] and is inconsistent with the wavelength dependence shown in Figure 9. Although substantial quenching of QDs takes place immediately in the presence of PDEAEM homopolymer, maximum quenching occurs several minutes after the initial mixing, as shown in Figure 10. The measured quenching dynamics are consistent with multiple time scales associated with static and dynamic processes but also reflect the unique aspects of the QD−polymer system. In this case, we infer that immediate quenching results from collisions among QDs and polymer molecules, but that static complexation of QDs and polymers requires additional time to reach equilibrium resulting in saturated quenching after several minutes. The concept of static quenching in this system is unusual as it is dominated by QD self-quenching interactions which are mediated by associations with polymer.

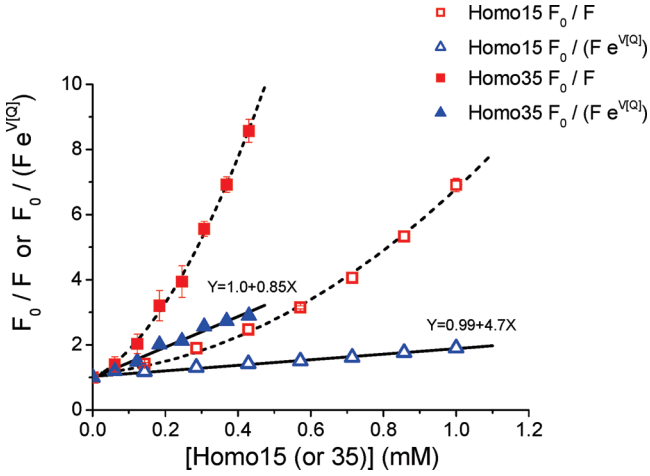

Figure 8. Quenching of QDs as a function of concentration of homopolymers (Homo15, Homo35). Squares show plots of quenching using the standard definition of F_0/F. Triangles show a rescaled version of quenching consistent with a Stern−Volmer model of static and dynamic quenching. The latter definition provides a linear fit to the data.

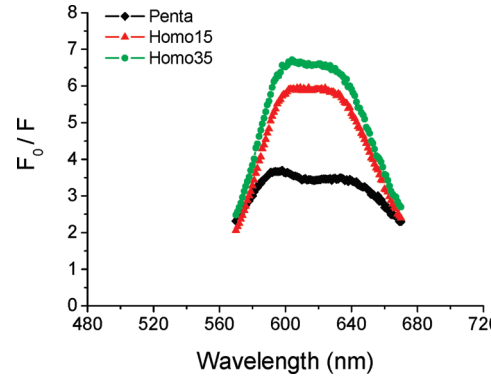

Figure 9. Wavelength-dependent quenching of QDs in the presence of various polymer quenchers.

CONCLUSIONS

We have shown that water-soluble Cys-capped CdSe−ZnS QDs are capable of sensing the dissociation of DNA/polymer polyplexes following exposure to chloroquine. Upon exposure to free pentablock copolymer and/or DNA, the QD fluorescence is quenched increasingly with concentration. The mechanism of fluorescence quenching was determined by exposing QDs to polymers and DNA individually and in various combinations. Studies with PDEAEM homopolymers suggested that tertiary amines were the functional groups responsible for quenching during exposure to the pentablock copolymer. However, the greatest quenching effect was observed when using pentablock copolymer, presumably due to its unique micellar conformation. QD fluorescence quenching was modeled using modified Stern−Volmer equations that account for static and dynamic quenching subject to modifications specific to DNA and PDEAEM. Studies with mixed

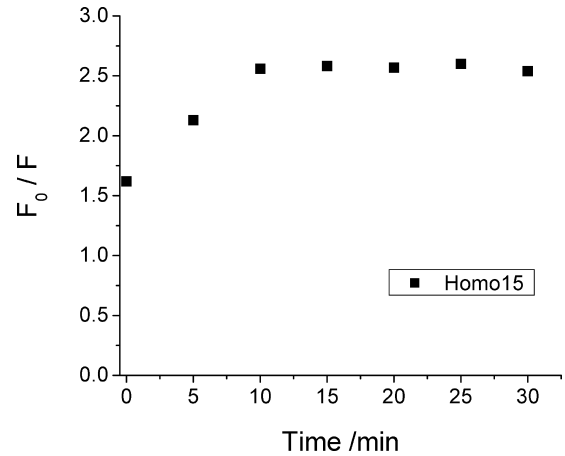

Figure 10. Homo15-induced quenching of QD with time. Fluorescence of QDs in the absence of quencher (Homo15), F_0, was measured at different time points to provide accurate control for corresponding measure of sample quenching. Equilibrium was reached in about 10 min.

populations of QDs showed that energy transfer plays a significant role in the overall quenching effect using PDEAEM and pentablock copolymer. These results collectively suggest that these QDs have the potential to sense the dissociation of DNA cargo from polyplexes both *in vitro* and within living cells.

MATERIALS AND METHODS

Materials. Hexadecylamine (HDA, 90%), hexamethyldisilathiane (TMS_2S), trioctyl phosphine (TOP, 90%), and diethylzinc (Et_2Zn) were purchased from Sigma-Aldrich (St. Louis, MO) and used as received. Cadmium acetylacetonate ($Cd(acac)_2$) and selenium shot (Se, 99.99%) were used as received from Strem Chemicals (Newburyport, MA). Trioctylphosphine oxide (TOPO, 98%) was obtained from Alfa Aesar (Ward Hill, MA) and used as received. L-Cysteine (≥99%) was purchased from Acros Organics and used as received. Chloroquine diphosphate salt was obtained from Sigma-Aldrich. Pluronic F127 [$(PEO)_{100}$-*b*-$(PPO)_{65}$-*b*-$(PEO)_{100}$] (where PEO represents poly(ethylene oxide) and PPO represents poly(propylene oxide)) was donated by BASF (Florham Park, NJ) and used without further modification. Chloroform and carbon disulfide (CS_2) were used as received from Fisher Scientific (Pittsburgh, PA). A 6.7 kb pGWIZ-luc (GeneTherapy Systems Inc., CA) plasmid was purified with Qiagen HiSpeed Maxi Kit (Qiagen, Valencia, CA).

Preparation of Water-Soluble QDs by Ligand Exchange. CdSe−ZnS core−shell QDs were synthesized using a method previously reported by Clapp *et al.*[28] and Howarth *et al.*,[29] with some minor modifications. Briefly, appropriate quantities of hexadecylamine (HDA) and trioctylphosphine oxide (TOPO, ~10−30 g) were melted in a three-neck round-bottom flask at ~150 °C followed by degassing under vacuum and purging with N_2 *via* a Schlenk line. The mixture was further heated above 300 °C, where cadmium acetylacetonate ($Cd(acac)_2$) and selenium precursor (1 M trioctylphosphine-coordinated selenium, TOP:Se) were rapidly injected by syringe into the flask through a rubber septum. The temperature was then abruptly reduced to 80 °C to arrest the nanocrystal growth and ensure a narrow size distribution of CdSe core particles. CdSe cores were subsequently overcoated with multiple ZnS layers (three or more) by dropwise addition of diethylzinc (Et_2Zn) and hexamethyldisilathiane ($(TMS)_2S$) at ~140 °C. The resulting core−shell QDs were allowed to stir and anneal at 80 °C overnight.

To render CdSe−ZnS QDs water-soluble, a biphasic ligand reaction and exchange procedure was employed which we have reported recently.[30] Briefly, CdSe−ZnS QDs, having been purified by three-fold precipitation in dry methanol, were resuspended in chloroform ($CHCl_3$). Carbon disulfide (CS_2) was added to the $CHCl_3$ organic layer containing the QDs. A second aqueous phase was added to the 20 mL glass reaction vial containing dissolved cysteine (Cys). During 24 h of vigorous stirring, CS_2 and Cys reacted to form dithiocarbamate (DTC) ligands having high affinity for the QD surface. The newly hydrophilic Cys-capped QDs were collected from the aqueous layer and further purified using a 50k MW cutoff membrane filter (Millipore, Billerica, MA) and PD-10 chromatography column (GE Healthcare, Piscataway, NJ).

Preparation of Pentablock Copolymers and Homopolymers. Poly(diethylaminoethylmethacrylate) (PDEAEM)/Pluronic F127 pentablock copolymers and PDEAEM homopolymers were synthesized *via* atom transfer radical polymerization (ATRP). The detailed procedure has been described elsewhere.[31]

Polyplex Formation. Appropriate amounts of pentablock copolymer in HEPES buffer and plasmid DNA in water were mixed at N/P (nitrogen/phosphorus) ratio of 20, followed by incubation at room temperature for 30 min to ensure complete complexation. Detailed investigation of the properties of polyplexes was reported elsewhere.[32,33]

Measurement of Fluorescence. The fluorescence spectra of QDs in the presence of pentablock copolymers, polyplexes, DNA, chloroquine, and homopolyemers were measured by a dual monochromator spectrofluorimeter (Fluoromax-4, Horiba Jobin Yvon) with excitation at 370 nm and slit widths of 3 nm (excitation and emission). To ensure an equilibrated interaction between QDs and other reagents, mixtures were allowed to incubate for 30 min following addition of QDs to each sample.

Acknowledgment. We would like to thank Dr. Mathumai Kanapathipillai for help with polymer synthesis. A.R.C. thanks Iowa State University startup funds for supporting this work.

REFERENCES AND NOTES

1. Alivisatos, A. P.; Gu, W. W.; Larabell, C. Quantum Dots as Cellular Probes. *Annu. Rev. Biomed. Eng.* **2005**, *7*, 55–76.
2. Medintz, I. L.; Uyeda, H. T.; Goldman, E. R.; Mattoussi, H. Quantum Dot Bioconjugates for Imaging, Labelling and Sensing. *Nat. Mater.* **2005**, *4*, 435–446.
3. Duan, H.; Nie, S. Cell-Penetrating Quantum Dots Based on Multivalent and Endosome-Disrupting Surface Coatings. *J. Am. Chem. Soc.* **2007**, *129*, 3333–3338.
4. Rajan, S. S.; Liu, H. Y.; Vu, T. Q. Ligand-Bound Quantum Dot Probes for Studying the Molecular Scale Dynamics of Receptor Endocytic Trafficking in Live Cells. *ACS Nano* **2008**, *2*, 1153–1166.
5. Biju, V.; Muraleedharan, D.; Nakayama, K.; Shinohara, Y.; Itoh, T.; Baba, Y.; Ishikawa, M. Quantum Dot−Insect Neuropeptide Conjugates for Fluorescence Imaging, Transfection, and Nucleus Targeting of Living Cells. *Langmuir* **2007**, *23*, 10254–10261.
6. Gao, X. H.; Cui, Y. Y.; Levenson, R. M.; Chung, L. W. K.; Nie, S. M. *In Vivo* Cancer Targeting and Imaging with Semiconductor Quantum Dots. *Nat. Biotechnol.* **2004**, *22*, 969–976.
7. Jaiswal, J. K.; Mattoussi, H.; Mauro, J. M.; Simon, S. M. Long-Term Multiple Color Imaging of Live Cells Using Quantum Dot Bioconjugates. *Nat. Biotechnol.* **2003**, *21*, 47–51.
8. Walther, C.; Meyer, K.; Rennert, R.; Neundorf, I. Quantum Dot-Carrier Peptide Conjugates Suitable for Imaging and Delivery Applications. *Bioconjugate Chem.* **2008**, *19*, 2346–2356.
9. Chen, H. H.; Ho, Y. P.; Jiang, X.; Mao, H. Q.; Wang, T. H.; Leong, K. W. Simultaneous Non-invasive Analysis of DNA Condensation and Stability by Two-Step QD-FRET. *Nano Today* **2009**, *4*, 125–134.
10. Bruchez, M.; Moronne, M.; Gin, P.; Weiss, S.; Alivisatos, A. P. Semiconductor Nanocrystals as Fluorescent Biological Labels. *Science* **1998**, *281*, 2013–2016.
11. Chan, W. C. W.; Nie, S. M. Quantum Dot Bioconjugates for Ultrasensitive Nonisotopic Detection. *Science* **1998**, *281*, 2016–2018.
12. Agarwal, A.; Vilensky, R.; Stockdale, A.; Talmon, Y.; Unfer, R. C.; Mallapragada, S. K. Colloidally Stable Novel Copolymeric System for Gene Delivery in Complete Growth Media. *J. Controlled Release* **2007**, *121*, 28–37.
13. Agarwal, A.; Unfer, R. C.; Mallapragada, S. K. Dual-Role Self-Assembling Nanoplexes for Efficient Gene Transfection and Sustained Gene Delivery. *Biomaterials* **2008**, *29*, 607–617.
14. Zhang, B.; Kanapathipillai, M.; Bisso, P.; Mallapragada, S. Novel Pentablock Copolymers for Selective Gene Delivery to Cancer Cells. *Pharm. Res.* **2009**, *26*, 700–713.
15. Remy-Kristensen, A.; Clamme, J.-P.; Vuilleumier, C.; Kuhry, J.-G.; Mely, Y. Role of Endocytosis in the Transfection of L929 Fibroblasts by Polyethylenimine/DNA Complexes. *Biochim. Biophys. Acta* **2001**, *1514*, 21–32.
16. Huth, U. S.; Schubert, R.; Peschka-Süss, R. Investigating the Uptake and Intracellular Fate of pH-Sensitive Liposomes by Flow Cytometry and Spectral Bio-Imaging. *J. Controlled Release* **2006**, *110*, 490–504.

17. Breuzard, G.; Tertil, M.; Goncalves, C.; Cheradame, H.; Geguan, P.; Pichon, C.; Midoux, P. Nuclear Delivery of NκB-Assisted DNA/Polymer Complexes: Plasmid DNA Quantitation by Confocal Laser Scanning Microscopy and Evidence of Nuclear Polyplexes by FRET Imaging. *Nucleic Acids Res.* **2008**, *36*, 12.
18. Xavier, J.; Singh, S.; Dean, D. A.; Rao, N. M.; Gopal, V. Designed Multi-Domain Protein as a Carrier of Nucleic Acids into Cells. *J. Controlled Release* **2009**, *133*, 154–160.
19. Moore, N. M.; Sheppard, C. L.; Sakiyama-Elbert, S. E. Characterization of a Multifunctional PEG-Based Gene Delivery System Containing Nuclear Localization Signals and Endosomal Escape Peptides. *Acta Biomater.* **2009**, *5*, 854–864.
20. Shen, G.; Fang, H. F.; Song, Y. Y.; Bielska, A. A.; Wang, Z. H.; Taylor, J. S. A. Phospholipid Conjugate for Intracellular Delivery of Peptide Nucleic Acids. *Bioconjugate Chem.* **2009**, *20*, 1729–1736.
21. Yang, S.; Coles, D. J.; Esposito, A.; Mitchell, D. J.; Toth, I.; Minchin, R. F. Cellular Uptake of Self-Assembled Cationic Peptide−DNA Complexes: Multifunctional Role of the Enhancer Chloroquine. *J. Controlled Release* **2009**, *135*, 159–165.
22. Erbacher, P.; Roche, A. C.; Monsigny, M.; Midoux, P. Putative Role of Chloroquine in Gene Transfer into a Human Hepatoma Cell Line by DNA Lactosylated Polylysine Complexes. *Exp. Cell Res.* **1996**, *225*, 186–194.
23. Cheng, J. J.; Zeidan, R.; Mishra, S.; Liu, A.; Pun, S. H.; Kulkarni, R. P.; Jensen, G. S.; Bellocq, N. C.; Davis, M. E. Structure−Function Correlation of Chloroquine and Analogues as Transgene Expression Enhancers in Nonviral Gene Delivery. *J. Med. Chem.* **2006**, *49*, 6522–6531.
24. Wang, M. F.; Dykstra, T. E.; Lou, X. D.; Salvador, M. R.; Scholes, G. D.; Winnik, M. A. Colloidal CdSe Nanocrystals Passivated by a Dye-Labeled Multidentate Polymer: Quantitative Analysis by Size-Exclusion Chromatography. *Angew. Chem., Int. Ed.* **2006**, *45*, 2221–2224.
25. Lakowicz, J. R. *Principles of Fluorescence Spectroscopy*, 3rd ed.; Springer: Berlin, 2006.
26. Somers, R. C.; Bawendi, M. G.; Nocera, D. G. CdSe Nanocrystal Based Chem-/Bio-Sensors. *Chem. Soc. Rev.* **2007**, *36*, 579–591.
27. Medintz, I. L.; Pons, T.; Trammell, S. A.; Grimes, A. F.; English, D. S.; Blanco-Canosa, J. B.; Dawson, P. E.; Mattoussi, H. Interactions between Redox Complexes and Semiconductor Quantum Dots Coupled *via* a Peptide Bridge. *J. Am. Chem. Soc.* **2008**, *130*, 16745–16756.
28. Clapp, A. R.; Goldman, E. R.; Mattoussi, H. Capping of CdSe-ZnS Quantum Dots with DHLA and Subsequent Conjugation with Proteins. *Nat. Protoc.* **2006**, *1*, 1258–1266.
29. Howarth, M.; Liu, W. H.; Puthenveetil, S.; Zheng, Y.; Marshall, L. F.; Schmidt, M. M.; Wittrup, K. D.; Bawendi, M. G.; Ting, A. Y. Monovalent, Reduced-Size Quantum Dots for Imaging Receptors on Living Cells. *Nat. Methods* **2008**, *5*, 397–399.
30. Zhang, Y.; Schnoes, A. M.; Clapp, A. R. Dithiocarbamates as Capping Ligands for Water-Soluble Quantum Dots. *ACS Appl. Mater. Interfaces* **2010**, *2*, 3384–3395.
31. Determan, M. D.; Cox, J. P.; Seifert, S.; Thiyagarajan, P.; Mallapragada, S. K. Synthesis and Characterization of Temperature and pH-Responsive Pentablock Copolymers. *Polymer* **2005**, *46*, 6933–6946.
32. Zhang, B.; Mallapragada, S. The Mechanism of Selective Transfection Mediated by Pentablock Copolymers; Part I: Investigation of Cellular Uptake *Acta Biometer.* In Press, doi:10.1016/j.actbio.2010.11.032.
33. Zhang, B.; Mallapragada, S. The Mechanism of Selective Transfection Mediated by Pentablock Copolymers; Part II: Nuclear Entry and Endosomal Escape *Acta Biometer.* In Press, doi:10.1016/j.actbio.2010.11.033.